Appl Nanosci (2014) 4:859–868
DOI 10.1007/s13204-013-0266-1

ORIGINAL ARTICLE

Antibiofilm efficacy of silver nanoparticles against biofilm of extended spectrum β-lactamase isolates of *Escherichia coli* and *Klebsiella pneumoniae*

Mohammad Azam Ansari · Haris M. Khan · Aijaz A. Khan · Swaranjit Singh Cameotra · Ruchita Pal

Received: 20 May 2013 / Accepted: 22 August 2013 / Published online: 6 September 2013

Abstract The ability of bacteria to develop antibiotic resistance and colonize abiotic surfaces by forming biofilms is a major cause of medical implant-associated infections and results in prolonged hospitalization periods and patient mortality. Different approaches have been used for preventing biofilm-related infections in health care settings. Many of these methods have their own demerits that include chemical-based complications; emergent antibiotic-resistant strains, and so on. Silver nanoparticles (AgNPs) are renowned for their influential antimicrobial activity. We demonstrate the biofilm formation by extended spectrum β-lactamases-producing *Escherichia coli* and *Klebsiella* spp. by direct visualization applying tissue culture plate, tube, and Congo red agar methods. Double fluorescent staining for confocal laser scanning microscopy (CLSM) consisted of propidium iodide staining to detect bacterial cells and concanavalin A-fluorescein isothiocyanate staining to detect the exopolysaccharides matrix were used. Scanning electron microscopy observations clearly indicate that AgNPs reduced the surface coverage by *E. coli* and *Klebsiella* spp. thus prevent the biofilm formations. Double-staining technique using CLSM provides the visual evidence that AgNPs arrested the bacterial growth and prevent the exopolysaccharides formation. The AgNPs-coated surfaces effectively restricted biofilm formation of the tested bacteria. In our study, we could demonstrate the complete antibiofilm activity AgNPs at a concentration as low as 50 μg/ml. Our findings suggested that AgNPs can be exploited towards the development of potential antibacterial coatings for various biomedical and environmental applications. These formulations can be used for the treatment of drug-resistant bacterial infections caused by biofilms, at much lower nanosilver loading with higher efficiency.

Keywords Antibiofilm · AgNPs · Con A-FITC · CLSM · Exopolysaccharides

M. A. Ansari (✉) · H. M. Khan
Nanotechnology and Drug Resistance Research Lab, Department of Microbiology, Jawaharlal Nehru Medical College & Hospital, Aligarh Muslim University, Aligarh 202002, Uttar Pradesh, India
e-mail: azammicro@gmail.com

A. A. Khan
Department of Anatomy, Jawaharlal Nehru Medical College & Hospital, Aligarh Muslim University, Aligarh 202002, Uttar Pradesh, India

S. S. Cameotra
Institute of Microbial Technology (IMTECH-CSIR), Sector 39-A, Chandigarh 160036, India

R. Pal
Advanced Instrumentation Research Facility, Jawaharlal Nehru University, New Delhi, India

Introduction

The widespread use of antibiotics both inside and outside of medicine is playing a significant role in the emergence of multi-drug-resistant bacteria. Antibiotic resistance is a type of drug resistance where a microorganism is able to survive exposure to an antibiotic (Goossens et al. 2005; Motta et al. 2003). Now a days, about 70 % of the bacteria that cause infections in hospitals are resistant to at least one of the drugs most commonly used for treatment. Some organisms are resistant to all approved antibiotics and they can only treat with experimental and potentially toxic drugs (Todar 2008). Extended spectrum β-lactamases (ESBLs)-producing microorganisms are very dynamic and

constitutes an increasing problem due to their hydrolyzing activity against extended spectrum third generation cephalosporins such as cefotaxime, ceftriaxone, ceftazidime, and the monobactam aztreonam often employed in the treatment of hospital-acquired infections (Romero et al. 2005; Dechen et al. 2009). The majority of ESBL-producing strains are *Enterobacteriacea*e members such as *Klebsiella pneumoniae*, *Klebsiella oxytoca*, and *Escherichia coli* (Ami et al. 2008).

In recent years, there has been considerable interest in the problems posed by the biofilm mode of bacterial growth. A biofilm is a population of cells growing on a surface and enclosed within an exo-polymer matrix that can restrict the diffusion of substances and bind antimicrobials. This will provide effective resistance of biofilm cells against large molecules such as antimicrobial proteins lysozyme and complement (Ishida et al. 1998). The ability of bacteria to form biofilms helps them to survive hostile conditions within host and is considered to be responsible for chronic or persistent infections (Costerton et al. 1999). Chronic infection associated with the use of medical devices may be established because of the ability of bacteria to adhere to inanimate surfaces. There is now widespread recognition of biofilms to human infection. Microbes attached to a surface are usually considered to be less susceptible to antimicrobial agents and are protected from the host immune response, giving rise to chronic infections that are notoriously difficult to eradicate (Lewis 2007). The armament of therapeutic agents available to treat bacterial infections today is restricted to antibiotics developed specially to kill or to stop the growth of individual bacteria (Sritharan and Sritharan 2004). In modern clinical microbiology, establishment of bacterial biofilms considered a pathogenicity trait during chronic infections (Sritharan and Sritharan 2004). The difficulty in eradicating a chronic infection associated with biofilm formation lies in the fact that biofilm bacteria are able to resist higher antibiotic concentration than bacteria in suspension (Gristina et al. 1987). Nanotechnology may provide the answer to penetrate such biofilms and reduce biofilm formation. Silver nanotechnology can prevent the formation of life-threatening biofilms on medical devices. Silver is one of the oldest known antimicrobials. Antimicrobial silver is now used extensively to combat organisms in wounds and burns. Although the literature reports some studies related to the antibacterial activity of AgNPs, to the authors' knowledge, there are very few studies concerning the effect of these particles against adhered cells and biofilms of ESBLs *E. coli* and *Klebsiella* spp. Therefore, the aim of the present study was to evaluate the antibiofilm potential of AgNPs against biofilms of ESBLs by Congo red, scanning electron microscopy (SEM) and double fluorescent staining confocal laser scanning microscopy (CLSM).

Materials and methods

Collection of samples

Clinical specimens of wounds, pus, urine, and blood were received from patients admitted in tertiary care hospital over a period of 6 months. All the samples were aseptically transported in nutrient broth within 45 min of sample collection.

Antibiotic susceptibility testing

Individual isolates were tested, based on the recommendations of the Clinical and Laboratory Standards Institute (CLSI 2006), by the Kirby–Bauer disc diffusion method for susceptibility to the following antibiotics: cefoperazone (Cs, 30 μg), cefoperazone–clavulanate (CsC, 75/10 μg), cefotaxime (Ce, 30 μg), ceftriaxone (Ci, 30 μg), ceftazidime (Ca, 30 μg), ceftazidime–clavulanate (CaC, 30/10 μg), gentamycin (G, 10 μg). Antibiotic discs used were procured by HiMedia (Mumbai, India).

Detection of ESBLs

During the present study, sensitivity disc of cefotaxime (30 μg), ceftazidime (30 μg), and ceftriaxone (30 μg) were used for screening of ESBL production. Diameter of zone of inhibition of growth was measured and interpreted according to CLSI criteria (CLSI 2006). The isolates with reduced sensitivity against two of four drugs mentioned above were interpreted as suspected ESBL producers.

Double disk synergy test

Phenotypic confirmation of these provisional ESBL producers was done by testing with sensitivity disc of ceftazidime and cefotaxime alone and in combination with clavulanic acid (10 μg) as recommended by CLSI (2006). The cefotaxime (30 μg) and cefotaxime–clavulanic acid (30/10 μg) disc were placed 20 mm apart on MHA plate. Similarly, the ceftazidime (30 μg) and ceftazidime–clavulanic acid (30/10 μg) disc were placed 20 mm apart. After incubating overnight at 37 °C, a $\geq$5 mm increase in the zone diameter for either antimicrobial agent, which was tested in combination with clavulanic acid versus its zone when tested alone, was interpreted as positive for ESBL (CLSI 2006).

Characterization of AgNPs

A stock solution of commercially available water-soluble AgNPs (5–10 nm) were procured from Nanoparticle Biochem, Inc. (Columbia, USA).

High-resolution transmission electron microscopy (HR-TEM) analysis of nanoparticles

The size and morphology of the nanoparticles were analyzed by HR-TEM. The sample was prepared by placing a drop of very dilute suspension of nanoparticles solution on carbon coated copper grid and allowed to dry by evaporation at ambient temperature and kept under a desiccator before loading them onto a specimen holder. The TEM measurements were performed at an accelerating voltage of 200 kV (Technai G2, FEI, Electron Optics, USA).

X-ray diffraction pattern of AgNPs

X-ray diffraction (XRD) pattern of AgNPs was recorded by Bruker D8 diffractometer using CuK_{α} radiation ($\lambda = 1.54056$ Å) in the range of $20° \leq 2\theta \leq 80°$ at 40 keV. The lattice parameters were calculated by the PowderX software. The particle size (D) of the sample was calculated using the Scherrer relationship:

$$D = \frac{0.9\lambda}{B\cos\theta}$$

where λ is the wavelength of X-ray, B is the broadening of the diffraction line measured half of its maximum intensity in radians, and θ is the Bragg's diffraction angle.

Detection of biofilm formation

Tissue culture plate method

The tissue culture plate (TCP) assay described by Christensen et al. (1985) is most widely used and was considered as standard test for detection of biofilm formation. 10 ml of Trypticase soy broth (TSB) with 1 % glucose was inoculated with a loopful of test organism from overnight culture on nutrient agar and was incubated at 37 °C for 24 h. The culture was further diluted 1:100 with fresh medium. 96-well flat bottom TCPs were filled with 0.2 ml of diluted cultures individually and were incubated at 37 °C for 24 h. Only sterile broth was served as blank. After incubation, gentle tapping of the plates was done. The wells were washed with 0.2 ml of PBS (pH 7.2) four times to remove free-floating bacteria. Biofilms which remained adherent to the walls and the bottoms of the wells were fixed with 2 % sodium acetate and stained with 0.1 % crystal violet. Excess stain was washed with deionized water and plates were dried properly. Optical densities (OD) of stained adherent biofilm were obtained with a micro ELISA auto reader at wave length 570 nm. Experiment was performed in triplicate and repeated thrice. Average of OD values of sterile medium was calculated and subtracted from all test values (Lewis 2001).

Tube method (TM)

A qualitative assessment of biofilm formation was determined as previously described by Christensen et al. (1982). Ten millilitres TSB with 1 % glucose was inoculated with a loopful of microorganism from overnight culture plates and incubated for 24 h at 37 °C. The tubes were decanted and washed with PBS 0.1 % (pH 7.3) and dried. Dried tubes were stained with crystal violet (0.1 %). Excess stain was removed and tubes were washed with deionized water. Tubes were then dried in inverted position and observed for biofilm formation.

Biofilm formation was considered as positive, when a visible film lined the wall and bottom of the tube. Ring formation at the liquid interface was not indicative of biofilm formation. Experiments were performed in triplicate and repeated three times.

Congo red agar method

Freeman et al. (1989) had described an alternative method of screening of biofilm formation; which requires the use of a specially prepared solid medium brain heart infusion broth (BHI) supplemented with 5 % sucrose and Congo red for screening the formation of biofilm. The medium was composed of BHI (37 gm/l), sucrose (50 gm/l), agar No. 1 (10 gm/l), and Congo red stain (0.8 gm/l). Congo red was prepared in the form of concentrated aqueous solution and it was autoclaved at 121 °C for 15 min, separately from other medium constituents. Following autoclave, the concentrated solution was added to agar which was previously cooled to 55 °C. Plates were inoculated and incubated aerobically for 24–48 h at 37 °C. Positive result was indicated by black colonies with a dry crystalline consistency. Weak slime producers usually remained pink, though occasional darkening at the centers of colonies was observed. A darkening of the colonies with the absence of a dry crystalline colonial morphology indicated an indeterminate result.

Scanning electron microscopy

Biofilms were assessed as previously described with or without AgNPs. Briefly, the cells were washed with PBS, fixed with 2.5 % glutaraldehyde, then fixed samples were subsequently washed again with PBS and dehydrated gently by washing in a series of ethanol alcohol (30, 50, 70, 80, 95, and 100 % for 10 min) at room temperature, and critical point drying was performed. Afterwards, cells were then oriented, mounted on the aluminum stubs, and coated with gold before imaging. The topographic features of the biofilms were visualized with a SEM (Carl Zeiss EVO 40, Germany) with accelerating voltage of 20 kV.

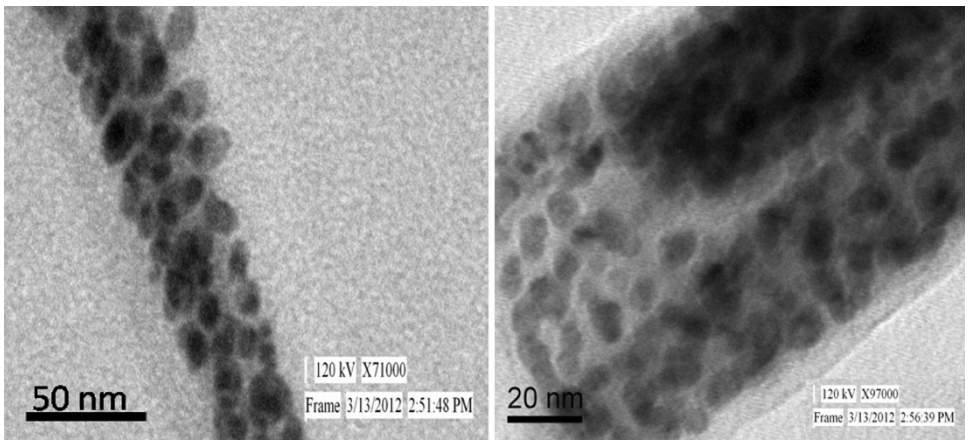

Fig. 1 HR-TEM micrograph of AgNPs

Confocal laser scanning microscopy

Biofilms for confocal analysis were grown on glass coverslips as previously described by Banas et al. (2001). Briefly, eight-well microtiter plate seeded with glass coverslips were incubated for 24 h at 37 °C in 5 ml of BHI with 5 % sucrose. The wells were inoculated with 100 µl of mid-exponential grown culture. After 24 h, the coverslips were removed and gently washed with sterile PBS and were then stained with 15 µM propidium iodide (Sigma) for 15 min at room temperature in order to detect red bacterial cells. After being washed in PBS, the cultures were incubated with 50 µg/ml of concanavalin A-conjugated fluorescein isothiocyanate (Con-A FITC-Sigma) for 15 min at room temperature to stain the glycocalyx matrix green. The propidium iodide was excited at 520 nm, the emission was monitored at 620 nm, and Con A-FITC was excited and monitored at 495 and 525 nm, respectively. Intact biofilms were examined non-destructively using a Fluoview FV 1000 Espectral Olympus CSLM (Olympus Latin America, Miami, FL, USA) equipped with a UPlanSApo 100X/1.40 oil UIS2 Olympus oil immersion lens. Then, for each sample, images from three randomly selected positions were obtained and analyzed using an Olympus Fluoview FV 1000.

Results

Characterization of silver nanoparticles

High-resolution transmission electron microscopy analysis revealed that the AgNPs were prominently spherical in morphology and monodisperse. It is evident that there is variation in particle sizes and the average size estimated was ~7 nm (Fig. 1).

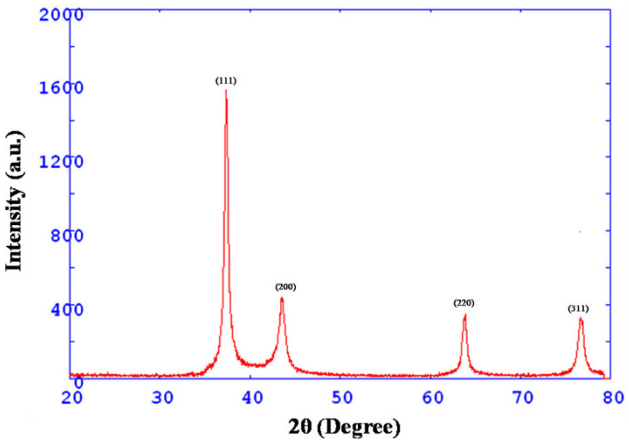

Fig. 2 XRD pattern of AgNPs employed in the study

XRD pattern of AgNPs

Figure 2 shows XRD data of the AgNPs. The peaks at $2\theta = 38.12°$, 44.35°, 64.56°, and 77.48° can be assigned to reflections from the (111), (200), (220), and (311) planes, respectively, of metallic silver in FCC phase. From geometry, it is clear that these individual particles are 6–7 nm in diameter. The high-resolution TEM data show crystal planes and this further supports XRD analysis for the crystalline nature of AgNPs.

Prevalence of bacterial isolates

A total of 46 strains were isolated from different clinical specimens like wounds, pus, and blood. Out of these; 40 (86.95 %) were *E. coli* and 6 (13.04 %) were *K. pneumoniae*. All strains of *E. coli* (40) and *K. pneumoniae* (6) were tested for ESBL production. There was a high frequency of ESBLs-positive *K. pneumoniae* isolation and all isolates of *K. pneumoniae* were positive for ESBLs, while 32 (80 %) isolates were ESBLs positive for *E. coli*. It was found that 10 (25 %) isolates of *E. coli* which were ESBLs producers showed resistance to all the drugs used in this study except

Imipenem. 18 (56.2 %) ESBLs-producing *E. coli* isolates showed maximum sensitivity for Gentamycin, while all ESBLs strains of *K. pneumoniae* were resistant to all drugs except Gentamycin (Table 1).

MIC and MBC of AgNPs

The MIC of AgNPs was found to be in the range 11.25–45 μg/ml for ESBL and non-ESBL *E. coli* (Table 2a), while the MIC for *Klebsiella* spp. were also observed in the range 11.25–45 μg/ml (Table 2b).

Screening of biofilm formation on Congo red agar

Table 3a shows that out of 40 isolates of *E. coli* and 6 of *Klebsiella* spp. tested for biofilm formation by Congo red agar (CRA) method, 26 (65 %) isolates of *E. coli*, 4 (66.67 %) isolates of *Klebsiella* spp. produced black colonies. However, only 14 (35 %) isolates of *E. coli* and 3 (50 %) isolates *Klebsiella* spp. colonies were black in color with dry crystalline consistency, which is indicative of biofilm formation.

Table 1 Antimicrobial susceptibility pattern of ESBL and non-ESBL bacterial isolates

Antibiotics	*E. coli* (40)		*Klebsiella* spp. (6)
	ESBL (32) (%)	Non-ESBL (8) (%)	ESBL (6) (%)
Gentamycin G	18 (56.2)	8 (100)	6 (100)
Cefotaxime Ce	4 (12.5)	6 (75)	0 (0)
Ceftriaxone Ci	6 (18.6)	8 (100)	0 (0)
Cefoperazone Cs	4 (12.5)	8 (100)	0 (0)
Cefoperazone + clavulanate CsC	16 (50)	8 (100)	0 (0)
Ceftazidime Ca	4 (12.5)	8 (100)	0 (0)
Ceftazidime + clavulanate CaC	16 (50)	8 (100)	6 (100)

Screening of biofilm formation by TCP method

Quantitative microtitre assay for biofilm formation was strongly positive in 8 (20 %) isolates of *E. coli* and 2 (33.33 %) *Klebsiella* spp., while the remaining isolates were either moderate adherent 14 (35 %) *E. coli* and 1 (16.67 %) or weak/non-biofilm producers 18 (45 %) *E. coli* and 3 (50 %) *Klebsiella* spp. (Table 3b).

Screening of biofilm formation by TM

Qualitative TM of biofilm screening of bacterial isolates showed that 18 (45 %) isolates of *E. coli* and 4 (66.67 %) isolates of *Klebsiella* spp. were positive for biofilm production (Table 3c). Most of the isolates showed thick blue ring at the liquid–air interface.

Characterization of antibiofilm activity of AgNPs on CRA plates

Biofilm formation is detected in many organisms synthesizing exopolysaccharides. Biofilm formation by *E. coli* and *Klebsiella* spp. were tested by growing the organism in Brain heart infusion agar supplemented with Congo red (BHIC) with and without AgNPs. When the colonies were grown without AgNPs in the medium, the organisms appeared as dry crystalline black colonies, indicating the production of exopolysaccharides, which is the prerequisite for the formation of biofilm (Fig. 3). Whereas when the organisms were grown on BHIC with AgNPs, the organisms did not survive. During the treatment with reduced concentrations of AgNPs (10 μg/ml), the organisms continued to grow, but AgNPs treatment has inhibited the synthesis of exopolysaccharides, indicated by the absence of dry crystalline black colonies (Fig. 3). It was found that at higher concentration of AgNPs inhibited bacterial growth by more than 98 %. When the exopolysaccharide synthesis is arrested, the organism cannot form biofilm. It

Table 2 MIC and MBC values of AgNPs tested against *E. coli* and *Klebsiella* spp.

(a) ESBL positive *E. coli* 32 (80 %)				Non-ESBL *E.* coli 8 (20 %)			
Isolates (%)	MIC μg/ml	Isolates (%)	MBC μg/ml	Isolates (%)	MIC μg/ml	Isolates (%)	MIC μg/ml
12.5	11.25	81.25	45.00	25	11.25	25	22.50
62.5	22.50	12.5	22.50	62.5	22.50	75	45.00
25	45.00	6.25	11.25	12.5	45.00	–	–
(b) ESBL positive *Klebsiella* spp. 4 (66.67 %)				Non-ESBL *Klebsiella* spp. 2 (33.33 %)			
Isolates (%)	MIC μg/ml	Isolates (%)	MIC μg/ml	Isolates (%)	MIC μg/ml	Isolates (%)	MIC μg/ml
25	11.25	25	22.50	50	11.25	25	22.50
75	22.50	75	45.00	50	22.50	75	45.00

Table 3 Screening of biofilm formation by clinical isolates of *E. coli* and *Klebsiella* spp. by (a) congo red agar (*CRA*), (b) tissue culture plate (*TCP*), and (c) Tube methods

(a) Colony appearance on (CRA)	*E. coli* (%)	*Klebsiella* spp. (%)
Pink/red (negative)	14 (35)	2 (33.33)
Black colonies without dry crystalline consistency (indeterminate)	12 (30)	1 (16.77)
Black colonies with dry crystalline consistency (positive)	14 (35)	3 (50.00)
(b) Biofilm production (TCP)	*E. coli* (%)	*Klebsiella* spp. (%)
Weak/Non (<0.120 OD)	18 (45)	3 (50.00)
Moderate (0.12–0.24 OD)	14 (35)	1 (16.67)
High (>0.24OD)	8 (20)	2 (33.33)
(c) Biofilm production (TM)	*E. coli* (%)	*Klebsiella* spp. (%)
0/1 (weak/non)	14 (35)	3 (50)
2+ (moderate)	12 (30)	1 (16.67)
3+ (strong)	6 (15)	2 (33.33)

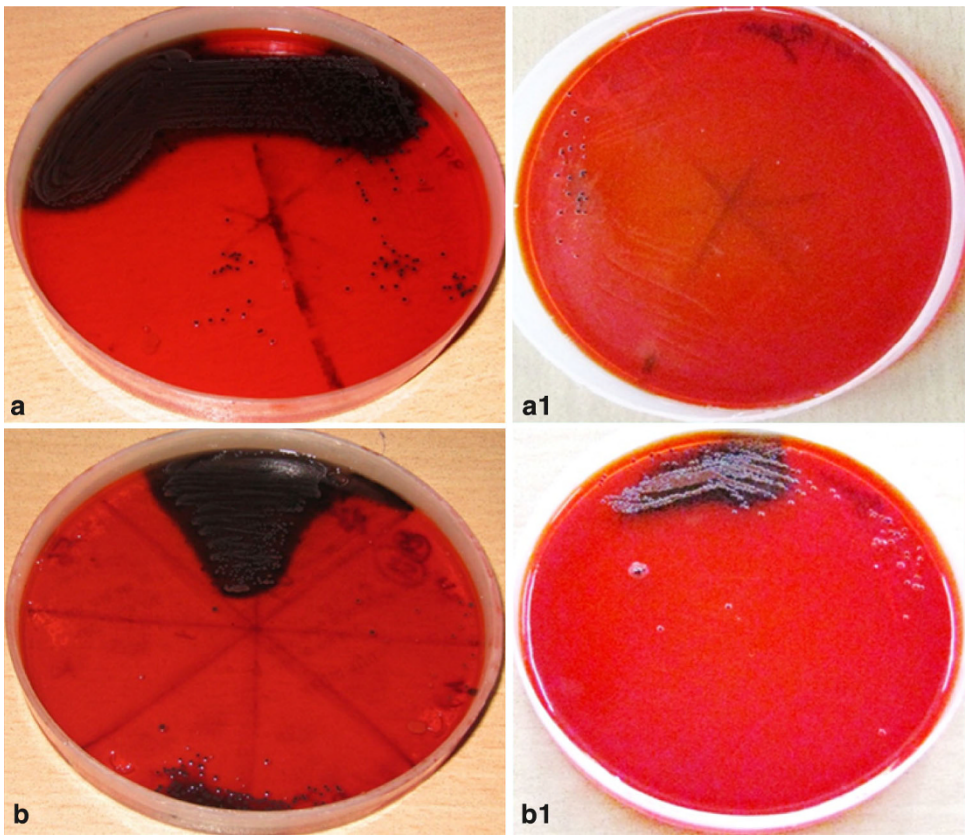

Fig. 3 Ability of the organisms was checked for biofilm formation in BHI agar supplemented with *Congo red*. The appearance of *black crystalline* colonies indicate the exopolysaccharide production by *E. coli* (**a**) and *Klebsiella* spp. (**b**), whereas the addition of 50 microgram/ml AgNPs blocked the exopolysaccharide synthesis by *E. coli* (**a1**) and *Klebsiella* spp. (**b1**) and also inhibited the growth of the organism itself

was also observed that 20 μg/ml of AgNPs significantly arrested biofilm formation without affecting viability, whereas 50 μg/ml completely blocked the biofilm formation and inhibited the growth of the organism itself.

Characterization of antibiofilm activity of AgNPs by CLSM

Confocal laser scanning microscopy analysis of biofilms formation by clinical isolates of *E. coli* (Fig. 4a) and *Klebsiella* spp. (Fig. 4b) was performed; to examine the effects of coating of AgNPs on biofilm architecture using AgNPs-coated glass coverslips in a 12-well microtiter plate. To visualize bacterial cells and the surrounding glycocalyx matrix (which is indicative of bacterial biofilm formation), double staining was performed using propidium iodide and ConA-FITC. Bacterial cells stained red and were easily identified by their size and morphologic features, when using propidium iodide. ConA-FITC binds to mannose residues resulting in green staining and indicating

the presence of a bacterial glycocalyx. Although, we observed the marked colocalization of green ConA-FITC staining with clusters of bacterial cells, the staining of the matrix was not homogeneously distributed. The presence of dark areas within the biofilm can be explained by the existing water channels, the heterogeneous production of the matrix and the types of exopolysaccharides within the biofilm, as well as the absence of ConA-FITC binding to the matrix. When CLSM images with red and green fluorescent intensities were superimposed, yellow color (green + red) revealed that the extracellular-ConA-FITC-reactive polysaccharide (green) was produced in the intracellular spaces (red), indicating thereby that extracellular polysaccharides were produced as a capsular component in biofilm. We observed that interconnected bacteria were encased in a scaffolding network composed of extracellular matrix, suggesting a three-dimensional architecture of biofilm formations. The micrographs suggest that the biofilm formed on uncoated AgNPs surfaces covered a larger surface area and had a definite architecture (Fig. 4a, b, panel 1). However, the biofilms formed on coverslips coated with AgNPs showed no or few spread

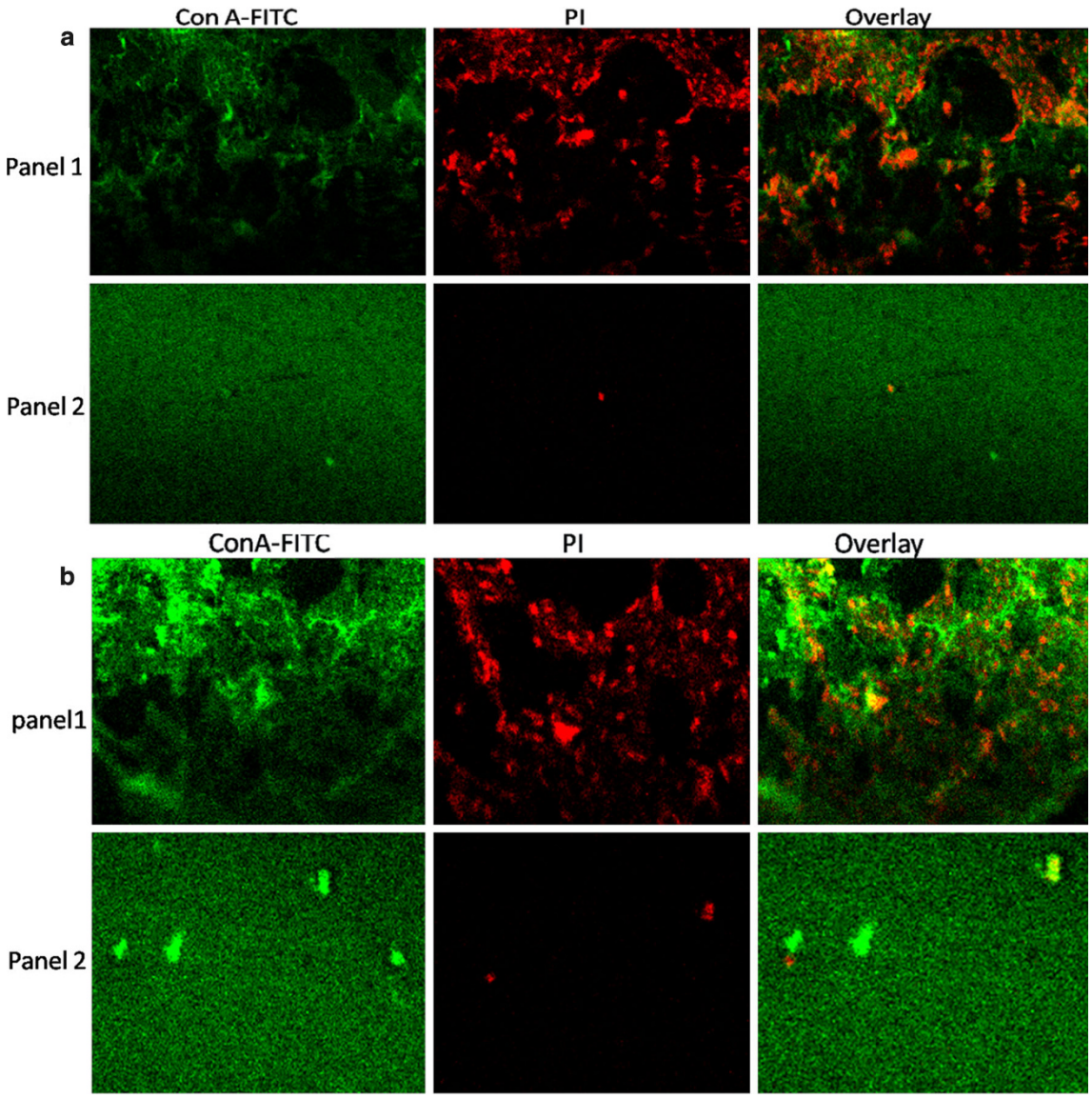

Fig. 4 CLSM micrographs of *E. coli* (**a**), *Klebsiella* spp. (**b**) biofilm. Panel 1 from *left* to *right* represents CLSM images of native biofilm (without AgNPs). Most of the bacteria were *rod-shaped*, with interconnected bacteria being encased in a scaffolding network composed of an extracellular matrix, suggesting a three-dimensional architecture of biofilm formations. *Red color* is PI staining of bacterial nucleic acids and green fluorescent staining (Con A-FITC) around bacteria indicates the presence of exopolysaccharides. Whereas, panel 2 from *left* to *right* represent CLSM images of *E. coli* (**a**) and *Klebsiella* spp. (**b**) biofilm treated with AgNPs and most of the cells were dead and no exopolysaccharides (*green fluorescent*) was observed. The number of live bacterial cells was reduced significantly, and the three-dimensional structure was also disrupted (×100).

cells with no distinct pattern of arrangement. The cells grown in the presence of 25 μg/ml AgNPs show a complete absence of clumped cells and were individually scattered over the surface rather than in any arrangement (Fig. 4a, b, panel 2). Uncoated coverslips surfaces supported a massive biofilm formation all bacterial cells, while AgNPs-coated surfaces dramatically restricted bacterial colonization.

Characterization of antibiofilm activity of AgNPs by SEM

The biofilm grown on glass slide for 24 h was observed using SEM. Irregularly shaped spaces resembling water channels were observed among dense structures and biofilm formed by the native strain have aggregated and clumped bacterial cells. The *E. coli* (Fig. 5a) cultures grown without AgNPs exhibit the expected normal cellular morphology with smooth cell surfaces. Under the same growth conditions but in the presence of different concentrations of AgNPs; *E. coli* (Fig. 5b–f) cells show changes in morphology and it was also examined that AgNPs inhibit bacterial colonization on the surfaces. More specifically, an obvious increase in the roughness of the cell surface suggested that it has been damaged by the nanoparticles. Microscope evaluation of the surfaces clearly shows that the AgNPs treated glass surfaces do not allow bacterial colonization and biofilm formation compared to the untreated controls. Untreated glass surfaces supported a massive biofilm formation, while AgNPs-treated glass surfaces show dramatically restricted bacterial colonization and biofilm formation (Fig. 5b–f). These results suggest that AgNPs are effective in restraining bacterial colonization of the surface.

Discussion

Biofilm development is an area of intense research and the components involved in development have been considered possible targets for therapy. Surprisingly little is known about the inhibitors of biofilm-forming ESBL pathogens. To date, there are few known antibiofilm compounds. Wood (2009) shown that several non-toxic antibiofilm (antivirulence) compounds exist for *E. coli* including brominated furanones, ursolic acid, indole derivatives and 5-fluorouracil. The mechanism of resistance of bacterial biofilms has yet to be elucidated but a potentially important factor is production of the glycocalyx which enables cells growing within the biofilm to evade host defences and the activity of antimicrobial agents (Costerton et al. 1987). In order to kill or remove biofilms, antimicrobials must penetrate the polysaccharide matrix to gain access to the microbial cells. Nanotechnology may provide the answer to penetrate such biofilms and reduce biofilm formation by the use of "nanofunctionalization" surface techniques to prevent the biofilm formation. The antibiofilm efficacy of AgNPs was investigated by growing the organism on CRA supplemented with and without

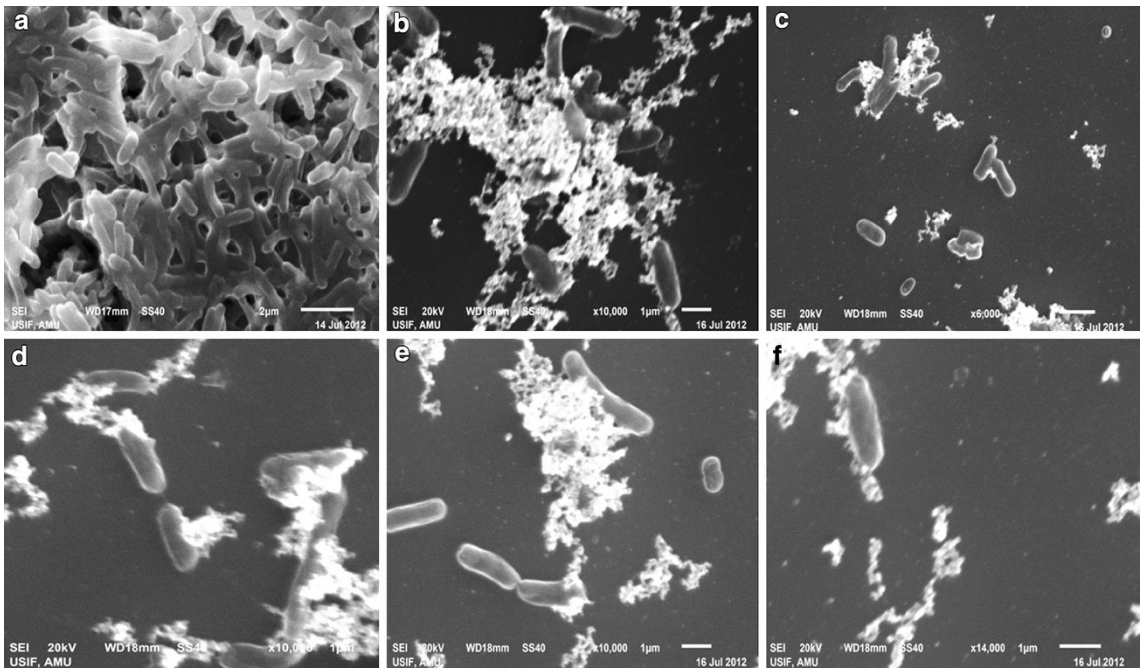

Fig. 5 SEM micrographs of *E. coli* biofilms developed on the glass slide surface at 24 h of incubation. Untreated (**a**), treated with (**b**) 10, (**c**), 20 (**d**) 30, (**e**) 40, and (**f**) 50 microgram/ml of AgNPs

AgNPs. When the colonies were grown without AgNPs, the organisms appeared as dry crystalline black colonies, indicating the production of exopolysaccharides, which is the prerequisite for the formation of biofilm (Fig. 3). Whereas when the organisms were grown with AgNPs, the organisms did not survive. Thus, when the exopolysaccharide synthesis is arrested, the organism cannot form biofilm. Similar results were also reported by Kalishwaralal et al. (2010) against *P. aeruginosa* and *S. epidermidis* biofilms and found that 100 nM of AgNPs resulted in a 95–98 % reduction in biofilm.

Based on these results we continued to address the mechanism of action of AgNPs on biofilm-forming bacterial species by applying CLSM and SEM. SEM was used to examine cell morphologies following exposure to the nanoparticles. *E. coli* cultures grown without nanoparticles exhibit the expected normal cellular morphology with smooth cell surfaces (Fig. 5a). Under the same growth conditions but in the presence of suspended AgNPs (20 µg/ml), *E. coli* cells showed changes in morphology (Fig. 5b–f). More specifically, an obvious increase in the roughness of the cell surface suggested that it has been damaged by the nanoparticles. EPS within *E. coli* biofilms was not detected by SEM. SEM observations clearly indicate that AgNPs reduced the surface coverage by *E. coli* biofilms (Fig. 5b–f). Our results are an agreement with previously reported antibiofilm activity of nanocrystalline silver by (Kostenko et al. 2010). They observed that nanocrystalline silver dramatically decreased viable cell numbers within the tested biofilms. The surface coverage by *E. coli* biofilms was reduced by the tested dressings by approximately 20 % after the first day.

The presence of biofilms on medical devices or surfaces can only be observed using a limited number of techniques. The reason why the demonstration of bacterial biofilms is challenging is because it is difficult to stain both the bacteria and glycocalyx. Furthermore, light and electron microscopy techniques require a dehydration process that reduces the total volume of the matrix and alters its architecture (Akiyama et al. 2003). For many applications, time lapse microscopy using CLSM is an ideal tool for monitoring at a spatial resolution of the order of micrometers, and allows the non-destructive study of biofilms through an examination of all the layers at different depths, thus making it is possible to reconstruct a three-dimensional structure (Lawrence and Neu 1999; Psaltis et al. 2007).

Therefore, to visualize the bacterial cells and the surrounding glycocalyx matrix (which is indicative of bacterial biofilm formation), we used this powerful technique CLSM to examine the effect of nanoparticles on glycocalyx matrix/exopolysaccharides synthesis; double staining was performed using propidium iodide and ConA-FITC. In case of untreated *E. coli* and *Klebsiella* spp. (Fig. 4a, b panel 1), PI stain bacterial nucleic acids and fluorescent red, while, green fluorescent (ConA-FITC) around bacteria indicates the presence of exopolysaccharides. Whereas, AgNPs-treated samples of *E. coli* and *Klebsiella* spp. (Fig. 4a, b panel 2) show that most of the cells were dead and no exopolysaccharides (green fluorescent) was observed. The number of live bacterial cells was reduced significantly, and the three-dimensional structure was also disrupted. We investigated that this inhibitory effect of AgNPs on the existing biofilm may be due to the presence of water channels though out the biofilm. Since in all biofilms water channels (pores) are present for nutrient transportation, AgNPs may directly diffuse through the exopolysaccharides layer through the pores and may impart antimicrobial function. Chaudhari et al. (2012) investigated the antibiofilm activity of AgNPs (51 nm) synthesized from *B. megaterium* and reported that AgNPs showed enhanced quorum quenching activity against *S. aureus* biofilm and prevention of biofilm formation which can be seen under inverted microscope. They concluded that AgNPs might be involved in neutralizing these adhesive substances, thus preventing biofilm formation.

Conclusion

However, the exact mechanism of action of AgNPs in biofilm-related studies is yet to be demonstrated. Kostenko et al. (2010) reported that Acticoat nanocrystalline silver has the highest antibiofilm efficacy compared to Aquacel silver and Silverlon and the silver concentration alone cannot account for the antibiofilm efficacy of the silver dressings. The type of silver species present also plays a role (Kostenko et al. 2010). The reduction of the silver particle to the nanoscale level increases the relative surface area, which provides higher Ag^{+} release rates than for elemental silver particles (Dunn and Edwards-Jones 2004). Moreover, nanoparticles have a higher capacity to attach to and penetrate bacterial membranes and accumulate inside cells, providing a continuous release of silver ions inside the cell (Rai et al. 2009; Kostenko et al. 2010). In the near future, the AgNPs may play major role in the coating of medical devices and treatment of infections caused due to highly antibiotic resistant biofilm. This study suggests that AgNPs have antibiofilm therapeutic potential, but further studies are still required namely regarding formulation and delivery means.

Acknowledgments The authors would like to acknowledge SAIF-DST, Department of Anatomy, All India Institute of Medical Sciences (AIIMS), New Delhi, for HRTEM and Advanced Instrumentation Research facility, Jawaharlal Nehru University, New Delhi, India for SEM and CLSM observation. Authors would like to thank the Indian

Council of Medical Research (ICMR), New Delhi-India, Grant Number 35/15/BMS-11 for their partial support and funding of this project.

Conflict of interest None declared.

References

Akiyama H, Hamada T, Huh WK et al (2003) Confocal laser scanning microscopic observation of glycocalyx production by *Staphylococcus aureus* in skin lesions of bullous impetigo, atopic dermatitis and pemphigus foliaceus. Br J Dermatol 148:526–532

Ami YV, Dogra JD, Kulkarni MH, Bhalekar PN (2008) Extended spectrum beta lactamase producing *Escherichia coli* and *Klebsiella pneumoniae* in diabetic foot infection. J Pathol Microbiol 51(3):370–372

Banas JA, Hazlett KRO, Mazurkiewicz JE (2001) An in vitro model for studying the contributions of the *Streptococcus mutans* glucan-binding protein-A to biofilm structure. Meth Enzymol 337:425–433

Chaudhari PR, Masurkar SA, Shidore VB, Kamble SP (2012) Effect of biosynthesized silver nanoparticles on *Staphylococcus aureus* biofilm quenching and prevention of biofilm formation. Intern J Pharm Bio Sci 3(1):222–229

Christensen GD, Simpson WA, Bisno AL, Beachey EH (1982) Adherence of slime-producing strains of *Staphylococcus epidermidis* to smooth surfaces. Inf Immun 37:318–326

Christensen GD, Simpson WA, Younger JA, Baddour LM, Barrett FF, Melton DM et al (1985) Adherence of coagulase negative *Staphylococci* to plastic tissue cultures: a quantitative model for the adherence of *Staphylococci* to medical devices. J Clin Microbiol 22:996–1006

CLSI (2006) Performance standards for antimicrobial susceptibility testing, Fifteenth Informational Supplement, CLSI document. M100-S16, vol 26-3; M7-A7, vol 26-2; M2-A9, vol 26-1. Wayne, PA

Costerton JW, Cheng KJ, Geesey GG, Ladd IT, Nickel JC, Dasgupta M et al (1987) Bacterial biofilms in nature and disease. Ann Rev Microbiol 41:435–464

Costerton JW, Stewart PS, Greenberg EP (1999) Bacterial biofilms: a common cause of persistent infections. Science 284:22–1318

Dechen CT, Das S, Adhiakari L, Pal R, Singh TSK (2009) Extended spectrum beta lactamases detection in gram negative bacilli of nosocomial origin. J Glo Inf Dis 1(2):22–28

Dunn K, Edwards-Jones V (2004) The role of Acticoat with nano crystalline silver in the management of burns. Burns 30:1–9

Freeman DJ, Falkiner FR, Keane CT (1989) New method for detecting slime production by coagulase negative *Staphylococci*. J Clin Pathol 42:872–874

Goossens H, Ferech M, Vander-Stichele R, Elseviers M (2005) Outpatient antibiotic use in Europe and association with resistance: a cross-national database study. Lancet 365:579–587

Gristina AG, Hobgood CD, Web LX, Myrvik QN (1987) Adhesive colonization of biomaterials and antibiotics resistance. Biomaterial 8:423–426

Ishida H, Ishida Y, Kurosaka T, Otani KS, Kobayashi H (1998) In vitro and in vivo activities of levofloxacin against biofilm-producing *Pseudomonas aeruginosa*. Antimicrob Agen Chemother 42:1641–1645

Kalishwaralal K, BarathManiKanth S, Pandian SRK, Deepak V, Gurunathan S (2010) Silver nanoparticles impede the biofilm formation by *Pseudomonas aeruginosa* and *Staphylococcus epidermidis*. Colloids Surf, B 79:340–344

Kostenko V, Lyczak J, Turner K, Martinuzzi TJ (2010) Impact of silver-containing wound dressings on bacterial biofilm viability and susceptibility to antibiotics during prolonged treatment. Antimicrob Agen Chemother 54(12):5120–5131

Lawrence JR, Neu TR (1999) Confocal laser scanning microscopy for analysis of microbial biofilms. Meth Enzymol 310:131–144

Lewis K (2001) Riddle of biofilm resistance. Antimicrob Agens Chemother 45(4):999–1007

Lewis K (2007) Persister cells, dormancy and infectious disease. Nat Rev Micro 5:48–56

Motta RN, Oliveia M, Megalhaes PSF, Dias AM, Aragao LP, Forti AC, Carvalho (2003) Plasmid mediated extended spectrum beta lactamase producing strains of enterobacteriaceae isolated from diabetes foot infections in a Brazilian diabetic centre. Bra J Inf Dis 7(2):1024–1032

Psaltis AJ, Ha KR, Beule AG, Tan LW, Wormald PJ (2007) Confocal scanning laser microscopy evidence of biofilms in patients with chronic rhinosinusitis. Laryngoscope 117(7):1302–1306

Rai M, Yadav A, Gade A (2009) Silver nanoparticles as a new generation of antimicrobials. Biotechnol Adv 27:76–83

Romero L, Lopez L, Bano JR, Martinoz M, Pascual A (2005) Long term study of frequency of *Escherichia coli* and *Klebsiella pneumoniae* isolates producing ESBLs. Euro Soc Clin Microbiol Inf Dis 11:625–631

Sritharan M, Sritharan V (2004) Emergings problems in the management of infectious diseases: the biofilms. Ind J Med Microbiol 22:140–142

Todar K (2008) Bacterial resistance to antibiotics. Textb Bacteriol 304:1421

Wood TK (2009) Insights on *Escherichia coli* biofilm formation and inhibition from whole-transcriptome profiling. Environ Microbiol 11(1):1–15